Evaporation of cosmological quark drops and relativistic radiative transfer

Luciano Rezzolla

Scuola Internazionale di Studi Avanzati, Trieste, Italy

John C. Miller

Scuola Internazionale di Studi Avanzati, Trieste, Italy

Department of Physics, University of Oxford, England

Osservatorio Astronomico di Trieste, Trieste, Italy

Abstract

We discuss the results of a full relativistic treatment of the hydrodynamics of disconnected quark regions during the final stages of the cosmological quark-hadron transition. In this study, which represents a further development of a previous analysis of the evaporation of cosmological quark drops, the effects of long range energy and momentum transfer via electromagnetically interacting particles are consistently taken into account. For this purpose, a set of relativistic Lagrangian equations describing the evolution of the strongly interacting fluids is coupled to a system of equivalent equations accounting for the hydrodynamics of the fluid of electromagnetically interacting particles. The complete set of equations has then been solved numerically and results are presented from this. The inclusion of relativistic radiative transfer produces significantly different results, with the formation of high density regions at the end of the drop evaporation being particularly relevant. A comparison is made with results obtained for the previous radiation-free model and the cosmological implications concerning baryon number concentrations are briefly discussed.

I. Introduction

A phase transition at which the cosmological plasma of free quarks and gluons was transformed into a plasma of light hadrons, is thought to have occurred early in the history of the Universe. The physical conditions for this transition to take place, date it back to a few microseconds after the Big-Bang, when the Universe had a mean density of the same order as nuclear matter ($\rho \sim 10^{15}$ g cm^{-3}), and a temperature of the order of $100 - 200$ MeV. The quark-hadron transition marks the end of the exotic physics of the very early Universe and the beginning of the era of processes and phenomena which have a direct counterpart in the high energy experiments now being carried out with modern accelerators. It is also the last of the early Universe phase transitions (at least within the standard picture) and so could be relevant both as a potential filter for the relics produced by previous transitions and also as a "best candidate" for the production of inhomogeneities which could have survived to later epochs.

It has not proved possible to determine the order of the transition directly from QCD but, rather, its determination depends on heavy lattice gauge calculations which rely on a number of simplifying assumptions and uncertain parameters. Because of this, any consistent modelling of the transition is immediately confronted by a major uncertainty concerning the order of the transition. It is relevant to note that while a continuous cosmological quark-hadron phase transition [1] would strongly prevent any dynamical production of primordial inhomogeneities [2], the occurrence of these seems to be a rather natural consequence of a first order transition. We here follow this latter scenario and investigate the hydrodynamical mechanisms which could lead to the production of inhomogeneities at the end of a first order cosmological quark-hadron transition. We note that this picture is, in fact, favoured by recent lattice computations which include the effects of two degenerate light u and d quarks and a heavier s quark (of up to 400 MeV) [3, 4, 5, 6], and clearly indicate the existence of a double state signal for the quark gluon plasma.

The aim of the present work is to discuss the final stages of the transition, which we define to be those when most of the strongly interacting matter in the Universe is already in the form of light hadrons. The temperature jump between the quark and hadron phases is then no longer extremely small and the rate at which the quark-gluon plasma is transformed is no longer controlled by the overall expansion of the Universe. The quark regions have become disconnected, with a mean separation comparable with the distance between bubble nucleation sites, and tend to assume a spherical shape under the effects of surface tension. A new dynamical time scale for the evolution of the transition then enters and this is directly related to the rate at which the quark drops shrink by losing material (*i.e.* by "evaporating").

In a recent paper [7], we have investigated and discussed the relativistic hydrodynamics of an isolated quark drop during the final stages of the transition in

the simplified picture where long range energy and momentum transfer is not included. In particular, we demonstrated the existence of a self-similar solution for the hydrodynamics of an isolated contracting spherical system and showed how this is, in fact, attained by an evaporating quark drop. A most important feature turned out to be the possibility of maintaining a constant quark phase compression during most of the stages of the drop evaporation. This had the consequence of preventing any large increase in the final value of the compression factor in the quark phase (the maximum relative increase computed was of the order of 40%), thus limiting the possibility of producing significant peaks of baryon number density as the drop disappears. In that work we considered the fluids of strongly interacting particles and that of electromagnetically interacting particles as always being coupled, neglecting the effective decoupling which must occur when the drop dimensions are comparable with the mean free path of the radiation particles.

In the present paper we extend the earlier study to the case where the effects of long range energy and momentum transfer are not neglected. To do this, a problem of relativistic radiative transfer needs to be solved at around the time of the decoupling between the two fluids, and an extended set of equations has to be solved numerically. In doing this we make use of the experience gained in the study of the related problem of long range energy and momentum transfer during the growth of a hadron bubble [8, 9], and also use the mathematical and numerical apparatus developed there.

The following is a summary of the organization of the paper. In Section II we review the essential features of the PSTF (Projected Symmetric Trace Free) tensor formalism [10] adopted for the solution of the relativistic radiative transfer; in Section III we introduce the set of hydrodynamical equations for the standard fluids and discuss how these couple to the equivalent ones for the radiation fluid. Section IV contains a discussion of the solution of the equations at the interface, where junction conditions and characteristic equations are solved. In Section V we briefly review the method for the numerical computation and the choice for the initial conditions. Numerical results are presented in Section VI and Section VII contains a brief discussion of their cosmological implications regarding the formation of baryon number inhomogeneities, which may be important in connection with primordial nucleosynthesis [11, 12] and also with the production of primordial magnetic fields [13]. Finally, conclusions are presented in Section VIII. We adopt units for which $c = \hbar = k_B = 1$; Greek indices are taken to run from 0 to 3 and partial derivatives are denoted with a comma.

2

II. Relativistic hydrodynamic equations for the radiation fluid

In the present Section and in the following one, we discuss the formulation of the system of equations which we use for studying the hydrodynamics of a contracting spherical drop, with radiative exchange of energy and momentum being included. We consider a "two-fluid" hydrodynamical model, and refer to the fluid composed of strongly interacting particles as the "standard fluid", and to the one composed of electromagnetically interacting particles (mainly photons, electrons, muons and their antiparticles) as the "radiation fluid". While the particles of the first fluid have a typical interaction scale length of the order of 1 fm, the particles of the second fluid have a larger interaction scale length, probably between 5×10^3 and 10^4 fm. Neutrinos, which have a much larger interaction scale length (of the order of 10^{13} fm = 1 cm), provide no effective contribution at the scale which we are mainly concerned with here and will in general be neglected.

Because of the difference between the scales of the internal interactions in the two fluids, it is possible to consider two asymptotic regimes during drop evaporation. When the drop has a radius R_s which is much larger than the mean free path (m.f.p.) of the radiation fluid particles λ, $(R_s \gg \lambda)$, it is reasonable to consider the two fluids as effectively coupled and behaving dynamically as a single fluid within each phase. In this case the treatment is simplified and the contribution of the different particle species can be taken into account by a suitable specification of the number of degrees of freedom in the equations of state for the two phases. On the other hand, when the drop has dimensions which are much smaller than the radiation m.f.p., $(R_s \ll \lambda)$, the opposite asymptotic regime is reached, where the drop has become effectively transparent to the radiation fluid particles. In this case, the decoupling between the two fluids can be taken into account by eliminating the number of degrees of freedom of the radiation fluid particles in the equations of state.

During drop evaporation there will be a stage (at $R_s \approx \lambda$) when the two fluids will start to decouple and long range exchange of energy and momentum will act in the direction of smoothing the discontinuities produced by the temperature difference between the two phases. In order to follow the effects of this transient process, it is necessary to adopt a treatment in which the radiative transfer problem and the hydrodynamical problem are solved simultaneously. For this purpose we have implemented the mathematical apparatus developed for studying the related problem of the progressive coupling between the standard fluid and the radiation fluid during the growth of a hadron bubble [8, 9] and the reader is referred to

this work for details of the derivation of the equations. We here limit ourselves to outlining the assumptions and main results of the PSTF tensor formalism which has been adopted.

As standard in radiation hydrodynamics, we need to solve the radiative transfer equation, which relates the properties of the radiation field (described by the photon distribution function) to the sources and sinks of the field and to the dynamics of the underlying medium when this is not stationary. For doing this, we make use of the frequency integrated PSTF tensor formalism in which the relativistic generalization of the radiative transfer equation is transformed into an infinite hierarchy of partial differential equations involving an infinite number of moments of the radiation intensity and of the field sources (the latter are referred to as source functions). A particularly attractive feature of the PSTF tensors, which are suitably defined at each point in the projected tangent space to the fluid four-velocity, is that they become effectively scalars when a global planar or spherical symmetry is present. Because of this, the PSTF formalism is particularly suitable for solving the radiative transfer problem for a contracting quark drop, since in this case, spherical symmetry enters as a natural consequence of the drop dynamics.

As in any infinite series expansion strategy, all of the properties of the radiation field are known exactly only when the infinite hierarchy of moments is determined. However, this is never possible in practice and a truncation at a finite order in the moment expansion is therefore necessary. This has two main consequences: firstly it introduces an overall intrinsic approximation in the determination of the radiation variables, and secondly it requires the introduction of a closure relation which specifies the value of the highest moment used in terms of lower ones. This supplementary equation, which should be derived on the basis of physical considerations, is somewhat heuristic and the form used for it is typically related to the specific problem under investigation.

As in [8, 9], we here truncate the infinite hierarchy of moments at the second order, thus making use of the first three scalar moments w_0, w_1 and w_2 and of the first two source functions s_0 and s_1. A truncation at the second order, which introduces an intrinsic overall error of the order of 15%, has a number of interesting and convenient features. Firstly, all of the scalar moments retained have direct physical interpretation, with w_0 and w_1 being the energy density and flux of the radiation in the rest frame of the standard fluid, and with w_2 representing the shear stress scalar of the radiation. Secondly, the moments used are only those appearing explicitly in the stress-energy tensor for the radiation fluid $T_R^{\alpha\beta}$, which, at any order, has the form

$$T_R^{\alpha\beta} = \mathcal{M}u^\alpha u^\beta + \mathcal{M}^\alpha u^\beta + \mathcal{M}^\beta u^\alpha + \mathcal{M}^{\alpha\beta} + \frac{1}{3}\mathcal{M}P^{\alpha\beta}, \tag{1}$$

where $P^{\alpha\beta}$ is the projection operator orthogonal to the fluid four-velocity u^α, and the first three PSTF moments $\mathcal{M}$, $\mathcal{M}^\alpha$, $\mathcal{M}^{\alpha\beta}$, are related to the equivalent scalar moments via the expressions

$$\mathcal{M} = w_0, \tag{2}$$

$$\mathcal{M}^\alpha = w_1 e_{\hat{r}}^\alpha, \tag{3}$$

$$\mathcal{M}^{\alpha\beta} = w_2 \left(e_{\hat{r}}^\alpha e_{\hat{r}}^\beta - \frac{1}{2} e_{\hat{\theta}}^\alpha e_{\hat{\theta}}^\beta - \frac{1}{2} e_{\hat{\varphi}}^\alpha e_{\hat{\varphi}}^\beta \right). \tag{4}$$

Here $(\mathbf{e}_{\hat{t}}, \mathbf{e}_{\hat{r}}, \mathbf{e}_{\hat{\theta}}, \mathbf{e}_{\hat{\varphi}})$ is the orthonormal tetrad carried by an observer comoving with the standard fluid. A particular advantage of truncating at the second order is that it is then possible to avoid the use of iterative methods for the derivation of the equations governing the hydrodynamics of the radiation fluid, which can instead be derived by means of the standard conservation laws of energy and momentum for the radiation fluid. We adopt Lagrangian coordinates comoving with the standard fluid and having their origin at the centre of the drop and write the (spherically symmetric) line element as

$$ds^2 = -a^2 dt^2 + b^2 d\mu^2 + R^2(d\theta^2 + \sin^2\theta \; d\varphi^2), \tag{5}$$

where μ is a comoving radial coordinate and R is the associated Eulerean coordinate. The PSTF equations can then be written as

$$-u_\alpha T_R^{\alpha\beta}{}_{;\beta} = s_0, \tag{6}$$

$$P_{\mu\alpha} \, T_R^{\alpha\beta}{}_{;\beta} = \frac{s_1}{b}, \tag{7}$$

$$w_2 = f_E w_0. \tag{8}$$

Equation (8) is the closure relation and specifies a connection between the second and the zeroth moments in terms of a variable Eddington factor f_E, which is an indicator of the degree of anisotropy of the radiation. This Eddington factor can take values ranging from 0 for complete isotropy (which, for example, is reached when the radiation fluid and the standard fluids are totally coupled) to 2/3 for

5

complete anisotropy (which could, in principle be reached when the two fluids are effectively decoupled). An expression for f_E has to be supplied and in doing this it is important that the correct asymptotic behaviour in any relevant limits is preserved and that the form chosen provides a suitably smooth join between the physical limits. Experience has shown [14, 15, 9] that as long as these requirements are met, results do not usually depend sensitively on the precise form used for f_E. As in [8, 9], we have here used for the Eddington factor the expression

$$f_E \equiv \frac{8u^2/9}{(1 + 4u^2/3)} \left(\frac{\lambda}{\lambda + R} \right),$$
(9)

which is the product of an exact expression accounting for the Doppler effects of motion with respect to a uniform radiation field, together with a corrective term (the one in the large parentheses) which provides the required physical join between the optically thin and optically thick limits. The scalar source functions s_0 and s_1 appearing in (6), (7), represent the sources or sinks of energy and momentum between the two fluids, and are expressed as

$$s_0 = \frac{1}{\lambda}(\epsilon - w_0) + (s_0)_{sc},$$
(10)

$$s_1 = -\frac{w_1}{\lambda},$$
(11)

where ϵ is the energy density for radiation in thermal equilibrium with the standard fluid (*i.e.* it is the equivalent of a local emissivity), and the term $(s_0)_{sc}$ expresses the contribution to the energy source due to non-conservative scatterings. Assuming a black-body expression for ϵ, we have

$$\epsilon = g_r \left(\frac{\pi^2}{30} \right) T_F^4,$$
(12)

with g_r being the number of degrees of freedom of the radiation fluid and T_F the local temperature of the standard fluid. Obtaining a suitable expression for $(s_0)_{sc}$ (which in general depends on the details on the problem under investigation) is particularly problematic in the present case where the number and the complexity of all the possible particle interactions prevent us from having an exact and simple expression. For this reason, we have adopted a phenomenological view and have expressed $(s_0)_{sc}$ in terms of the simple absorption and emission factor

$$(s_0)_{sc} = \frac{\alpha_2}{\lambda}(\epsilon - w_0),$$
(13)

where α_2 is an adjustable coefficient ranging between zero and one. Within a cosmological context it is reasonable to assume $\alpha_2 \approx 1$; a discussion of the differences caused by varying α_2 will be presented in Section VI.

Expressing equations (6) and (7) explicitly in terms of our metric, we obtain the following two equations of relativistic radiation hydrodynamics

$$(w_0),_t + \frac{a}{b}(w_1),_\mu + \frac{4}{3}\left(\frac{b,_t}{b} + \frac{2R,_t}{R}\right)w_0 + \frac{2a}{b}\left(\frac{a,_\mu}{a} + \frac{R,_\mu}{R}\right)w_1 + \left(\frac{b,_t}{b} - \frac{R,_t}{R}\right)w_2 = as_0, \tag{14}$$

$$(w_1),_t + \frac{a}{b}\left(\frac{1}{3}w_0 + w_2\right),_\mu + \frac{4a,_\mu}{3b}w_0 + 2\left(\frac{b,_t}{b} + \frac{R,_t}{R}\right)w_1 + \frac{a}{b}\left(\frac{a,_\mu}{a} + \frac{3R,_\mu}{R}\right)w_2 = as_1, \tag{15}$$

which, together with equation (8) provide a consistent description of the transfer of energy and momentum via the radiation fluid. During the final stages of the evaporation (*i.e.* for $R_s \ll \lambda$), the drop medium is locally optically thin and the energy density of the radiation fluid becomes uniform in the Eulerean frame. Under these circumstances (which are similar to those encountered in the early stages of bubble growth [9]), there is a tendency for numerical instabilities to appear, related to near cancellation problems and to almost diverging expressions in the characteristic form of equations (14) and (15). Experience has shown that a satisfactory numerical solution of the above equations is then possible only if they are rewritten in terms of new variables, defined by the following transformations

$$\tilde{w}_0 = w_0 - (w_0)^* = w_0 - \left(1 + \frac{4}{3}u^2\right)(w_0)_N, \tag{16}$$

$$\tilde{w}_1 = w_1 - (w_1)^* = w_1 + \frac{4}{3}u\Gamma(w_0)_N, \tag{17}$$

$$\tilde{w}_2 = w_2 - (w_2)^* = w_2 - \frac{8}{9}u^2(w_0)_N, \tag{18}$$

where

$$u = \frac{1}{a}R,_t, \tag{19}$$

$$\Gamma = \frac{1}{b}R,_\mu = \left(1 + u^2 - \frac{2GM}{R}\right)^{1/2}. \tag{20}$$

7

Here u is the radial component of fluid four velocity in the associated Schwarzschild (Eulerian) frame, Γ is the general relativistic analogue of the Lorentz factor and M a generalized mass function. The new "tilde" variables are expressed as differences between the standard moments and the expressions for these moments resulting from considering the motion of the fluid relative to a uniform radiation field having energy density $(w_0)_N$ in the Eulerean frame. This will here coincide with the initial value of the radiation energy density in the hadron phase, which we have therefore taken as the reference value. Making use of (16)–(18), it is then possible to obtain the following transformed radiation hydrodynamics equations [9]

$$
(\tilde{w}_0)_{,t} + a\tilde{w}_0 \left[\frac{1}{R^2} \left(\frac{4}{3} + f_E \right) (uR^2)_{,R} - \frac{3uf_E}{R} \right] + \frac{\Gamma}{aR^2} (\tilde{w}_1 a^2 R^2)_{,R}
$$
$$
+ a\frac{4}{3R} (w_0)_N \left[f_E (\frac{3}{4} + u^2) - \frac{2}{3}u^2 \right] \left[\frac{1}{R}(uR^2)_{,R} - 3u \right] + as_0
$$
$$
- \frac{4}{3} a(w_0)_N G \left[4\pi uR \left(2p - e - \frac{w_0}{3} + 2w_2 - \frac{u}{\Gamma}w_1 \right) - \frac{M}{R} \left(2u_{,R} + \frac{u}{R} \right) \right]
$$
$$
- \frac{4\pi aGR}{\Gamma} \left(\frac{4}{3}w_0 + w_2 \right) w_1 = 0 , \tag{21}
$$

$$
(\tilde{w}_1)_{,t} + 2\tilde{w}_1 \frac{a}{R}(uR)_{,R} + a\Gamma \left(\frac{\tilde{w}_0}{3} + \tilde{w}_2 \right)_{,R} + \Gamma \left(\frac{4}{3}\tilde{w}_0 + \tilde{w}_2 \right) a_{,R} + \frac{3a\Gamma\tilde{w}_2}{R}
$$
$$
+ as_1 + \frac{4}{3}a(w_0)_N \Gamma G \left[4\pi R \left(p + \frac{w_0}{3} + w_2 - \frac{u}{\Gamma}\ w_1 \right) + \frac{M}{a^2 R^2}(a^2 R)_{,R} \right]
$$
$$
- \frac{8\pi aGRw_1{}^2}{\Gamma} = 0 . \tag{22}
$$

where ρ is the *relative compression factor*, and e and p are the energy density and the pressure of the standard fluids. Note that it has been convenient here to replace the the partial derivatives with respect to μ by the equivalent derivatives with respect to R and that, for compactness, the radiation variables which are multiplied by the gravitational constant G are not transformed according to (16)–(18). Equations (21), (22) represent our final form of the hydrodynamical equations for the radiation fluid and need to be solved together with the corresponding hydrodynamical equations for the combined fluids, which will be discussed in the next Section.

III. Relativistic hydrodynamic equations for the standard fluid

The formal derivation of the hydrodynamical equations for the standard fluids is more standard. For this purpose in fact, it is possible to make use of the ordinary conservation equations for energy and momentum of the combined fluids (*i.e.* standard fluid plus radiation fluid) together with the continuity equation for the standard fluid. The equations which are then obtained, can be rewritten in a more familiar form by combining them with the Einstein field equations expressed in terms of the metric (5) and of a "total" stress-energy tensor (the sum of the one for the radiation fluid and of the one for the standard fluid). The set of equations is then [8]

$$u,_t = -a\left[\frac{\Gamma}{b}\left(\frac{p,_\mu + bs_1}{e+p}\right) + 4\pi G R\left(p + \frac{1}{3}w_0 + w_2\right) + \frac{GM}{R^2}\right], \tag{23}$$

$$\frac{(\rho R^2),_t}{\rho R^2} = -a\left(\frac{u,_\mu - 4\pi G b R w_1}{R,_\mu}\right), \tag{24}$$

$$e,_t = w\rho,_t - as_0, \tag{25}$$

$$\frac{(aw),_\mu}{aw} = -\frac{w\rho,_\mu - e,_\mu + bs_1}{\rho w}, \tag{26}$$

$$M,_\mu = 4\pi R^2 R,_\mu\left(e + w_0 + \frac{u}{\Gamma}w_1\right), \tag{27}$$

$$b = \frac{1}{4\pi R^2 \rho}, \tag{28}$$

$$w = \frac{(e+p)}{\rho}, \tag{29}$$

where a and b are the metric coefficients and w is the specific enthalpy of the standard fluids. The compression factor ρ expresses the variation in the proper volume of comoving elements of the standard fluid and for a classical standard fluid it can be replaced by the rest mass density. The set of equations (19)–(20) and (23)–(29) needs to be supplemented with equations of state for both phases of the strongly interacting matter. For small net baryon number and taking the hadronic medium to

9

consist of massless point-like pions, it is appropriate to describe the hadron plasma as an ultra-relativistic fluid, for which

$$e_h = (g_h + g_r) \left(\frac{\pi^2}{30} \right) T_h^4 \ , \qquad\qquad p_h = \frac{1}{3} e_h \ , \qquad (30)$$

while the quark phase can be effectively described by the *Bag model* equation of state

$$e_q = (g_q + g_r) \left(\frac{\pi^2}{30} \right) T_q^4 + B \ , \qquad p_q = (g_q + g_r) \left(\frac{\pi^2}{90} \right) T_q^4 - B \ , \qquad (31)$$

where $B = (\pi^2/90)(g_q - g_h)T_c^4$ is the "bag" constant, T_c is the critical temperature for the transition and g_q, g_h, g_r represent the number of effective degrees of freedom of the quark matter, the hadronic matter and the radiation particles respectively. Note that equations (30)–(31), (with $g_q = 37$, $g_h = 3$, and $g_r = 9$), apply when one considers the standard fluids and the radiation fluid as totally coupled, which is the case when the drop has dimensions $R_s \gg \lambda$. However, at the decoupling, and for all the subsequent stages of the drop evaporation, they need to be corrected by removing the additional number of degrees of freedom of the radiation fluid particles.

Equations (23)–(31), together with equations (19)–(22) and (8) represent the full system of hydrodynamical equations in the presence of long range energy and momentum transfer via electromagnetically interacting particles. However, the numerical solution of these equations must necessarily take into account the presence of a discontinuity between the phases of the strongly interacting matter at the drop surface. For this reason an appropriate treatment needs to be made of the conditions at the phase interface, and the way this has been accomplished is illustrated in the next Section.

IV.   Solution at the interface

The presence of an interface dividing the two phases of the strongly interacting matter introduces a number of complications when the set of the hydrodynamical equations discussed in the previous Sections is to be solved numerically. A first complication is related to the nature of the drop surface and to the way in which it should be described. Given the lack of detailed knowledge of the microphysics within the phase interface and the fact that the width of the interface is generally small

compared with the typical radial scale of the problem, it is convenient to treat it as a discontinuity surface across which rapid variations in the fluid variables occur. It is then possible to join the solution of the hydrodynamical equations on either side by imposing a number of relativistic junction conditions. For the particular case of a discontinuity surface with associated physical properties, (a non-vanishing stress energy tensor and an intrinsic curvature), the junction conditions can best be derived using the Gauss–Codazzi formalism [16, 17, 9]. Assuming that the surface tension σ is independent of temperature, ($\sigma = \sigma_0 T_c^3$, with $0 \leq \sigma_0 \leq 1$), the conservation of energy and momentum across the interface are expressed as

$$[(e+p)ab]^{\pm} = 0, \tag{32}$$

$$[eb^2\dot\mu_S^2 + pa^2]^{\pm} = -\frac{\sigma f^2}{2}\left\{\frac{1}{ab}\frac{d}{dt}\left(\frac{b^2\dot\mu_S}{f}\right) + \frac{f,_\mu}{ab} + \frac{2}{fR}(b\dot\mu_S u + a\Gamma)\right\}^{\pm}, \tag{33}$$

where $[A]^{\pm} = A^+ - A^-$, $\{A\}^{\pm} = A^+ + A^-$, μ_S is the interface location, $\dot\mu_S = d\mu_S/dt$, $f = (a^2 - b^2\dot\mu_S^2)^{1/2}$ and the superscripts $^{\pm}$ indicate quantities immediately ahead of and behind the interface. Note that the energy density and the pressure appearing in (32), (33) are the sum of those for the standard fluids and for the radiation fluid when these are totally coupled. At the decoupling however, and for all the following stages of the drop evaporation, it is necessary to supplement the equations (32), (33) (which will then refer to the standard fluids only), with the equivalent junction conditions for energy and momentum of the radiation fluid. Assuming that there is no interaction of the radiation fluid with the matter in the phase interface, the energy and momentum junction conditions for the radiation are then just the continuity conditions

$$\left[ab\dot\mu_S\left(\frac{4}{3} + f_E\right)\tilde w_0 - (a^2 + b^2\dot\mu_S^2)\tilde w_1 + (w_0)_N\left\{ab\dot\mu_S\left(1 + \frac{4}{3}u^2\right)\left(\frac{4}{3} + f_E\right)\right.\right.$$
$$\left.\left.+\frac{4}{3}u\Gamma(a^2 + b^2\dot\mu_S^2)\right\}\right]^{\pm} = 0 , \tag{34}$$

$$\left[\left\{a^2\left(\frac{1}{3} + f_E\right) + b^2\dot\mu_S^2\right\}\tilde w_0 - 2ab\dot\mu_S\tilde w_1\right.$$
$$\left.+(w_0)_N\left\{\left(1 + \frac{4}{3}u^2\right)\left[a^2\left(\frac{1}{3} + f_E\right) + b^2\dot\mu_S^2\right] + \frac{8}{3}abu\Gamma\dot\mu_S\right\}\right]^{\pm} = 0. \tag{35}$$

Other supplementary junction conditions follow from continuity across the interface of the metric quantities R, dR/dt, and ds

11

$$[R]^{\pm} = 0, \tag{36}$$

$$[au + b\dot{\mu}_s\Gamma]^{\pm} = 0, \tag{37}$$

$$[a^2 - b^2\dot{\mu}_s^2]^{\pm} = 0, \tag{38}$$

and from the time evolution of the mass function M

$$\frac{d}{dt}[M]^{\pm} = 4\pi R_s^2 \left[b\Gamma\dot{\mu}_s \left\{ \left(e + w_0 + \frac{u}{\Gamma}w_1 \right) \right\} - au \left\{ p + \left(\frac{1}{3} + f_E \right) w_0 + \frac{\Gamma}{u}w_1 \right\} \right]^{\pm}, \tag{39}$$

where the initial jump in mass across the interface is taken to be $[M]^{\pm} = 4\pi R_s^2\sigma$.

The concept of the phase interface as a perfect discontinuity surface needs careful interpretation in the context of a numerical calculation and in this case it is important to bear in mind that the interface should not be considered as strictly infinitesimal. In the present situation, in which the computer code follows the drop evaporation with an increasing spatial resolution through a number of orders of magnitude in radius, the interface should be thought of as having an effective width which is always smaller than the minimum length scale resolvable on the grid. This means that the numerical code will treat as discontinuous any change in the physical variables which cannot be resolved on the grid. This feature is particularly relevant at the decoupling, because at that stage the long range energy and momentum transfer introduces features of the flow on length scales which were not previously resolved when the standard fluids and the radiation fluid were considered as coupled. When the decoupling is allowed to start, the effective width of the phase interface is abruptly decreased to that appropriate for the strongly interacting matter alone and, as a consequence, changes across it which were previously discontinuous are allowed to smooth down and assume the profiles produced by the radiative transfer. In nature, the change between the two different situations is progressive and regular, but when described on an finite grid, it occurs discontinuously. Doing this requires particular care and in the next Section we discuss the details of the computational strategy which has been implemented in order to perform this change.

A further complication regarding the solution at the interface arises because of the dynamical properties of the drop surface treated as a reaction front. General

considerations about the nature of the transition [18, 19, 17] lead us to consider the transition as taking place by means of a weak deflagration front (*i.e.* by means of a discontinuity surface moving subsonically relative to the media both ahead and behind) [20, 21]. Weak deflagrations are intrinsically under-determined and require the specification of one additional condition giving the rate at which the quark matter is transformed into hadrons at the phase interface [21]. A simple and satisfactory expression can be obtained by setting the hydrodynamical flux F_H into the hadron region equal to the net thermal flux F_T into it

$$F_H = -\frac{aw\dot{\mu}_S}{4\pi R_S^2 (a^2 - b^2 \dot{\mu}_S^2)} = \left(\frac{\alpha_1}{4}\right)(g_h + g_r)\left(\frac{\pi^2}{30}\right)(T_q^4 - T_h^4) = F_T, \qquad (40)$$

where α_1 is an accommodation coefficient ($0 \leq \alpha_1 \leq 1$) containing information about the "transparency" of the phase interface to the thermal flux and is, at least in principle, calculable from theory.

It is very important to ensure that the correct causal structure is preserved when following the motion of a weak deflagration front as a discontinuity surface. A careful numerical investigation reveals that the only satisfactory way of accomplishing this is by making use of a characteristic method in which the system of partial differential equations is rewritten as a system of ordinary differential equations along specific curves in the space-time (the characteristic curves). The correct causal connection is then preserved as the characteristic curves are the world-lines along which information propagates through the media. We here make use of the same system of characteristic equations employed for the growth of a hadronic bubble and for compactness their lengthy expressions will not be repeated here (we refer the reader to [8, 9], where the details of their mathematical derivation is also given). Figure 1 shows the Lagrangian space-time configuration of the characteristic curves adjacent to the interface for evolution of the system from time level t to a subsequent time level $t + \Delta t$, with different line types distinguishing the different types of fluid. Note that, the gradients of the corresponding characteristics on the two sides of the phase interface can be different and that the difference between the sound speeds in the radiation fluid $[(1/3 + f_E)^{1/2}]$ and in the standard fluid (c_s), is greatly magnified in the figure.

Figure 1. The configuration of characteristic curves near the phase interface drawn in the Lagrangian coordinate frame.

13

As discussed above, the solution of the hydrodynamical equations at the phase interface is rather complicated and requires great care. However, once the set of radiation fluid and standard fluid hydrodynamical equations is solved along the characteristic curves (which are shown schematically in Figure 1) and the relevant junction conditions are imposed across the phase interface, a consistent numerical evolution of a weak deflagration front can then be computed.

V.   Numerical strategy and initial conditions

For following the evaporation of a quark-gluon drop and taking into account the progressive exchange of energy and momentum which at a certain stage will take place between the radiation fluid and the strongly interacting fluids, we have here made use of the experience and numerical codes developed for studying the related problems of radiative transfer for a growing hadron bubble [9] and of evaporation of a quark drop in the absence of long range energy and momentum transfer [7]. The result of this has produced a code which embodies the main features of the previous ones and we will briefly describe this here, referring the reader to the previous papers for further details.

As with its predecessors, the present code makes use of a composite numerical technique in which a standard Lagrangian finite-difference method is used to solve the hydrodynamical equations in the bulk of each phase, while a system of characteristic equations and a set of junction conditions are solved in the regions adjacent to the phase interface. The grid is Lagrangian and spherically symmetric with its origin at the centre of the drop. In order to follow the solution over a number of orders of magnitude in the spatial coordinate μ, the grid has variable spacing with the width of each successive zone being twice that of the previous one (*i.e.* $\Delta\mu_{j+1/2} = 2\,\Delta\mu_{j-1/2}$), apart from the two central zones which have equal width.

The specification of the initial conditions for the system of hydrodynamical equations has been guided by the existence of a self-similar solution for an isolated contracting physical system which was demonstrated in [7]. When there is no intrinsic length scale influencing the problem (as in the case of an isolated evaporating spherical drop for which surface tension is not yet playing a significant role), it is possible to write the set of hydrodynamical equations in terms of a single dimensionless independent variable and to find a similarity solution. The time evolution of the system is scale independent and reproduces itself at any instant. It is important to stress that this is a general feature of the similarity solution and holds for any dimensions of the system satisfying the above assumptions.

However, in the case of an evaporating quark drop during the cosmological phase transition, we do not expect the self-similarity to hold at all stages. Rather, it is necessary to establish an interval in the drop dimensions within which such self-similar behaviour is expected to take place. While the lower limit in the drop radius can easily be estimated from the magnitude of the surface tension σ associated with the phase interface (the surface tension introduces a natural length scale and the drop evaporation is no longer scale free when surface effects become relevant), the definition of the upper limit is more uncertain. In this case, it is necessary to determine an initial scale at which the quark drops can be considered physically disconnected, so that the distance between the centers of two neighbouring drops is larger than the sum of their respective "sonic radii" (see [7] for a definition). The value of this is not yet established and its determination would require a detailed hydrodynamical study of the intermediate stages of the transition, which we consider to be the ones after the hadron bubbles have coalesced and the quark regions have started to become disconnected. Simple geometrical considerations suggest that the mean separation between quark regions at bubble coalescence would be of the order of the mean separation of bubble nucleation sites (*e.g.* between 1 cm and 10^2 cm). Bearing in mind the uncertainty in this, we here take a conservative view and consider a quark drop of initial dimensions $R_{s,0} = 10^5$ fm, much below the above range. Considering such a small quark drop implies restricting our analysis to the very final stages of the transition, but it is then that the self-similarity is expected to break down and a change in the hydrodynamical evolution is expected to occur.

As initial conditions for the time evolution with the full hydrodynamical equations we therefore use the general form of the self-similar solutions, which is determined once the degree of supercooling in either one of the two phases has been established. It is worth noticing that the supercooling does not need to be extremely small as is the case during bubble percolation and coalescence. In fact, during the very final stages of the transition considered here, the quark volume fraction in the Universe has become very small and the confinement processes are no longer able to supply the energy necessary to maintain the increased hadron volume fraction at essentially T_c against the cooling produced by the expansion of the Universe [22]. All of the models which we present here refer to a quark drop having initial temperature $\hat{T}_q = T_q/T_c = 0.998$, surrounded by a hadron plasma at initial temperature $\hat{T}_h = T_h/T_c = 0.990$. A degree of supercooling of 1% in the hadron phase is, in our view, reasonable and allows numerical simulations to be performed within acceptable time costs. Moreover, it should be noted that results obtained with a smaller degree of supercooling (*e.g.* down to 0.1%) show only minimal overall differences for e, ρ and w_0 (always below a few percent). The situation is different if the degree of

15

supercooling is chosen to be *larger*. In this case, which probably has no cosmological relevance, the hydrodynamical evolution can be rather different and would follow the lines discussed in [7].

As mentioned in Section IV, an important feature of the present simulations is the transition between total coupling of the radiation and standard fluids and their effective decoupling. While in nature this process would take place in a rapid but gradual way, the start of it is necessarily discontinuous when simulated by means of a numerical calculation on a grid. For this reason it has been necessary to introduce a free parameter R_d, referred to as the "decoupling radius", fixing the drop radius at which the change is made from one regime to the other. For drop radii $R_s > R_d$ the two fluids are considered as totally coupled and moving as a single fluid. The phase interface is taken to have a width related to the m.f.p. of the radiation fluid particles and the characteristics of the radiation fluid are taken to coincide with the ones of the standard fluids. In practice the coupling is treated by adding the number of degrees of freedom of the radiation fluid particles to the number of degrees of freedom in the two phases of the strongly interacting matter and by setting to zero the contribution of the source functions s_0 and s_1 and the energy flux w_1. Also, the jump in w_0 at the interface is then calculated in terms of that for e. Conversely, for drop radii $R_s < R_d$ the two fluids are considered as not being totally coupled and the calculation of the radiation fluid variables adjacent to the interface is made using the radiation characteristics which are now distinct from those of the standard fluids. At this stage the radiation fluid evolves separately from the standard ones and long range energy and momentum transfer can start to take place.

It is worth pointing out that while in the above procedure the decoupling between the two fluids *starts* in a discontinuous manner, the decoupling in itself is *gradual* and is governed by the radiation hydrodynamic equations. The abrupt switch is certainly an approximation but, as discussed in next Section, it is a rather good one and numerical results show that the hydrodynamical evolution quickly recovers from the perturbation introduced by the sudden decoupling.

VI.   Numerical results

A.   The standard parameters

This Section is devoted to the presentation of the results obtained from the numerical integration of the hydrodynamical equations for the radiation and the standard fluids. We first present results for a standard set of the parameters of the problem and will discuss later the changes introduced when these parameters are allowed to vary. We here consider an isolated quark drop of initial radius $R_{s,0} = 10^5$ fm, surrounded by a hadron plasma at temperature $\hat{T}_h = 0.99$, and to which is associated a phase interface with surface tension parameter $\sigma_0 = \sigma/T_c^3 = 1$. (We assume $T_c = 150$ MeV). Moreover, we consider the phase interface as a perfect black-body (*i.e.* $\alpha_1 = 1$) and the non conservative scattering contribution in the first source function as maximal (*i.e.* $\alpha_2 = 1$). The decoupling radius is related to the m.f.p. of the radiation fluid particles and we here set $R_d = \lambda = 10^4$ fm.

Figures 2 and 3 show the time evolution of the radial component of the Eulerian four-velocity u and the energy density e of the standard fluids. The phase interface is represented by the vertical discontinuity, with the quark phase always being to the left of it and with the different curves referring to different stages during the contraction. The decoupling is allowed to start at a drop radius of 10^4 fm; as can be seen from the graphs, the solution is not particularly perturbed by the new conditions and quickly returns to a regular behaviour.

Figure 2. Time evolution of u, the radial component of the fluid four-velocity in the Eulerian frame. The quark phase is to the left of the vertical discontinuity. The decoupling between the radiation fluid and the standard fluids is allowed to start at $R_s = 10^4$ fm

Figure 3. Time evolution of the profile of the energy density e in the standard fluid.

These graphs are quite similar to the ones presented in [7] even though in this case the self-similar solution during the contraction is more weakly preserved after the decoupling. When the drop reaches dimensions comparable with the intrinsic

length scale $\sigma/w_q \approx 10^2$ fm, the self-similar behaviour is irreversibly lost and the evaporation then proceeds through the accelerated stages already observed in [7]. This is related to the contribution of the surface tension which has become overwhelming and produces a compression within the quark phase with a consequent temperature increase. Despite the reduced dimensions of the drop surface, the increased temperature jump between the two phases of the strongly interacting matter is able to preserve a considerable hydrodynamical flux away from the surface (the outward velocity is increased), thus allowing for an increasingly rapid evaporation which ends with the complete disappearance of the drop. Note that the treatment of the phase interface as a discontinuity surface is no longer correct when the drop radius reaches 1 fm and so our results for the smallest radii should only be treated as indicative.

Figures 4 and 5 show the time evolution of the radiation energy density w_0 and of the radiation energy flux w_1. Before the decoupling starts, w_0 obviously follows the self-similar evolution of the energy density of the standard fluids and the energy and momentum transfer between the two types of fluid is so efficient that they can be considered as in local thermodynamic equilibrium, giving ($w_1 = 0$). The situation changes when the drop becomes smaller then 10^4 fm. At this stage the decoupling starts and this has the effect of smearing out the step in the radiation energy density which was present before. Now the radiative transfer is able to carry away the energy stored within the radiation fluid in the quark phase.

As can be seen from the small diagrams in Figures 4 and 5, which show the evolution of w_0 and w_1 immediately after the decoupling has started, this process is quite rapid and before the drop radius has decreased by one order of magnitude, the radiation energy density profile has flattened out, equalizing with the value at infinity. The energy flux w_1 deviates from zero and becomes positive as soon as the decoupling starts and then progressively decays as the step in the radiation energy density is smeared out. This process is somewhat similar to the rapid release of the radiative energy contained within an optically thick, hot but non-emitting gas sphere which suddenly starts to become optically thin and is allowed to emit.

Figure 4. Time evolution of the radiation energy density w_0. The dashed curves are the result of dominant Doppler effects at the very end of the drop evaporation. The curves in the small diagram show the rapid evolution of energy density immediately after the decoupling has started.

Figure 5. Time evolution of radiation energy flux w_1. The curves in the small diagram show the rapid increase of the energy flux immediately after the decoupling has started.

The dashed curves in Figure 4 correspond to the very final stages of the drop evaporation (*i.e.* for drop dimensions of the order of a few fm). The increase in the radiation energy density which is seen there is related to the motion of the Lagrangian observers with respect to an essentially uniform radiation field and therefore has a pure Doppler nature (it can be shown that under these circumstances $w_0 \simeq (1 + 4u^2/3)(w_0)_N$ and $w_1 \simeq -(4\Gamma u/3)(w_0)_N$, [8]). Note that Doppler contributions are always present after the decoupling and are more evident in the energy flux, where they enter at the first order in u and are responsible for the increasing negative flux observed for drop radii smaller than 10^3 fm.

Some of the most interesting effects produced by the decoupling between the radiation fluid and the standard fluids regard the evolution of the compression factor ρ. As discussed in [7], a key property of the self-similar solution is that of preserving the values of the compression factor in the two phases of the strongly interacting matter. This reflects a perfect balance between the competing effects of the compression which would tend to be produced by the reduction in size of the quark drop and the evaporation processes which extract matter from it. As pointed out in [7], an increase in the compression within the quark phase is possible only when the self-similar solution is broken and this can occur either when the long range energy and momentum transfer takes place or, later on, when the drop radius becomes comparable with the intrinsic length scale related to the surface tension. If the decoupling between the radiation fluid and the standard fluids is neglected, (as in [7]), the compression produced is purely hydrodynamical and this takes place only during the very final stages of the drop evaporation. In that case, the relative increase of ρ^+, (the compression factor immediately ahead of the phase interface), at the end of the contraction of a standard quark drop with $\sigma_0 = 1$ and initial $\hat{T}_h = 0.99$, was computed to be of the order of 40%.

The situation changes dramatically if the radiative transfer between the standard fluids and the radiation fluid is consistently taken into account. Figure 6 shows the time evolution of the compression factor in both phases of the strongly interacting matter. With the magnified scale it is not possible to see the initial values of the compression factors which are $\rho_h = 0.253$ for the hadron phase and $\rho_q = 1.0$ for the quark phase, (our reference value). It is evident that as soon as the decoupling is allowed to take place at 10^4 fm, the compression within the quark phase starts to

19

increase progressively and, at the end of evaporation, it has reached values which are more than two orders of magnitude larger (an increase of $\sim 5 \times 10^4$ % !). The small diagram in Figure 6 traces the values of the compression just ahead of the phase interface (ρ^+) and just behind it (ρ^-).

Figure 6. Time evolution of standard fluid compression factor ρ. The curves in the small diagram represent the values of the compression factor immediately ahead of the phase interface (ρ^+) and immediately behind it (ρ^-).

The explanation for this striking behaviour is related to the fact that the long range radiative transfer is able to extract energy from within the quark phase without extracting the strongly interacting matter. As a consequence, the relation between the compression factor and the pressure (and hence between the compression factor and the temperature) is altered and the evaporation evolves in a radically non-adiabatic manner. The main effect produced by the radiative transfer is then that of reducing the specific entropy of the quark-gluon plasma, so that it is possible to enhance the quark compression without significantly changing its temperature.

It is interesting that the growth in the quark compression factor continues to occur also *after* the radiation energy density in the quark phase has been levelled down to the value in the hadron phase and the outward energy flux from the quark phase has become very small (*i.e.* even for $R_s < 10^3$ fm). This is due to the fact that when the energy density of the radiation fluid within the quark phase has reached the same value as in the hadron phase, there is a local temperature difference between the radiation fluid and the quark-gluon plasma which drives a very small but finite energy flux from the quark plasma into the radiation fluid, where it is then redistributed very efficiently. In this way the process of entropy extraction from the quark phase is able to operate even when the outward radiation energy flux from the quark phase is very small.

A limit to this mechanism is, of course, introduced by the intrinsic dimensions of the drop and by the length scale for the interactions of the particles of the radiation fluid. If the drop is too small, it becomes effectively transparent to the radiation particles and the entropy extraction is no longer efficient; at this stage the decoupling between the two fluids can be considered to be *complete*. For the typical quark drop under consideration here, this happens at about 10^2 fm, where the increase in the compression factor temporarily slows down (see the small diagram in Figure 6). At

this stage the solution would become self-similar again, but for the fact that the quark drop is now small enough for the surface tension to take over and dominate the final stages of the evaporation, producing the last compression enhancement. In the next Section it will be shown that it is possible to recover the self-similar solution again after the total decoupling has taken place if a suitable choice of the decoupling radius and of the m.f.p. λ is made (Figure 11).

A special comment should be made concerning a result which we consider to be particularly important. As discussed before, our treatment of the long range energy and momentum transfer between the radiation fluid and the standard fluids leads to an increase in the compression factor of the *quark* phase by about two orders of magnitude. It should be kept in mind, however, that this peak value is limited to a very small volume (of the order of 1 fm^3) and that it would be dispersed by the rarefaction wave following the complete disappearance of the drop (see [7] for a description of the rarefaction wave and Section VII for further discussions). As a consequence, if a relic inhomogeneity from the transition is to be investigated, this should rather concern the compression seen in the *hadron* phase before the disappearance of the drop.

Figure 7 shows the final profile of the compression factor ρ computed when the quark drop has reached a radius of 1 fm. It is interesting to note that besides the large peak in the quark phase, the compression factor has been increased also in the hadron phase, where it appears as a plateau of comparatively smaller magnitude. However, if one selects a vertical scale with greater resolution and normalizes the values of the compression factor to the background hadron compression (see the small diagram of Figure 7), it is clear that the plateau does indeed have a specific profile, with a maximum about two orders of magnitude larger than the background value. More important, the hadron compression extends over a much larger length scale, which coincides with the interaction length scale of the radiation fluid particles. Figures 6 and 7 could give a misleading impression as they seem to show that the most important effect is the compression increase in the quark phase whereas, in fact, the relative compression increase in the hadron phase is also substantial and is more significant in that it extends over a volume which is twelve orders of magnitude larger.

Figure 7. Final profile of the compression factor ρ; the computation has been stopped when the quark drop has a radius of 1 fm. The small diagram shows, with a different vertical resolution, the same profile after it has been normalized to the value of the hadron compression at infinity.

The compression increase in the hadron phase is not produced directly by the radiation, but rather results from the fact that "over-compressed" quark fluid elements (with decreased specific entropy) give rise to "over-compressed" hadron fluid elements after they have undergone the phase transformation in accordance with the junction condition (32). (Note that the entropy *increase* which naturally occurs across the phase interface is much smaller that the *decrease* introduced by the radiation fluid, so that fluid elements in the hadron phase near the drop have smaller specific entropy than those far from it). A key point to stress is that the over-compressed hadron plasma is in pressure balance (and therefore in temperature balance) with the surrounding hadron medium. This is a consequence of the decrease of specific entropy which took place while the fluid elements concerned were still inside the drop. At the end of the transition a spherical region of over-compressed hadron plasma is left behind which is in equilibrium with the surrounding medium. This is the region where a baryon number concentration could be produced and this would then only be dispersed by neutron diffusion on the time scale relevant for that. The consequences of this result for the production of baryon number inhomogeneities at the end of the transition will be discussed in Section VII.

B.   The parameter space

In this Section we discuss the changes introduced for the drop evaporation by variation of the set of the parameters within the allowed parameter space. We start by commenting on the hydrodynamical evolution of a quark drop for which the coefficient α_1, which relates the hydrodynamical flux to the thermal flux in the hadron phase, is not equal to unity as in the case of a perfect black-body surface. In general, reducing α_1 has the effect of decreasing the "transparency" of the drop surface to the phase transformation and therefore of slowing down the drop evaporation and favoring the long range energy and momentum transfer away from the quark phase.

Figure 8. Compression factors immediately ahead of and behind the phase interface when the radius of the quark drop has decreased to 1 fm, as a function of the adjustable coefficient α_1. The dashed curves extrapolate the numerical results to very small values of α_1, for which computations are not possible.

Figure 8 shows the variation, as a function of α_1, of the compression factors immediately ahead of and behind the phase interface when the radius of the quark

drop has decreased to 1 fm (the other parameters are left unchanged from the values discussed in the previous Section). While the solid curves fit points obtained by single computations, the dashed curves are an extrapolation of these to values of α_1 for which the computations would have been exceedingly time consuming (the computational time tends to infinity as α_1 tends to zero). It is interesting to notice that the formation of high compressions in the quark and hadron phases is a general feature and that the relative increase of the compression factors in both phases can easily be of six or seven orders of magnitude, thus giving a stronger cosmological relevance to this process.

Let us now consider the changes brought about by variation of the non-conservative scattering coefficient α_2 in the energy source moment (13). As mentioned in Section II, rough estimates indicate that $\alpha_2 \approx 1$ in the present cosmological scenario, but it is nevertheless interesting to consider situations for smaller values of α_2. It is obvious that a larger non-conservative scattering coefficient will enhance the efficiency of the radiative transfer processes and, in turn, the formation of compressed regions of the strongly interacting fluids.

Figure 9. Compression factor immediately ahead of the phase interface for computations with different values of the adjustable coefficient α_2. The small diagram shows the equivalent curves for the compression factor immediately behind the phase interface.

As shown in Figure 9, where results of computations performed with five different values of α_2 are presented, the hydrodynamical evolution is not qualitatively changed and although a value of $\alpha_2 = 1$ maximizes the compression, a relative compression increase (at the end of the drop evaporation) of about two orders of magnitude is present also in the total absence of the scattering contribution.

All of the results discussed so far are from simulations in which the decoupling between the radiation fluid and the standard fluids was allowed to start at a "decoupling radius" R_d equal to the m.f.p. λ of the strongly interacting particles. While such a choice is suggested by elementary considerations, there is no reason to exclude slightly smaller or larger values of R_d and it was interesting to consider the changes introduced for a decoupling started at $R_d/\lambda \neq 1$.

Figure 10. Compression factor immediately ahead of the phase interface when the radius of the quark drop has decreased to 1 fm, as a function of the decoupling radius R_d. The vertical axis is normalized to the value of ρ^+ obtained for $R_d = \lambda$. The solid line fits points obtained by single numerical simulations and the small diagram magnifies the results for small values of the decoupling radius.

Figure 10 collects the results of this investigation presenting the values of the final quark compression (at $R_s = 1$ fm), for different values of the decoupling radius. The value of ρ^+ presented in the diagram is normalized to the value obtained for $R_d = \lambda$; $R_d = 1.2 \ \lambda$ is the largest value for which a satisfactory numerical solution could be obtained, but $R_d = \lambda$ leads to a more regular behaviour of the hydrodynamical quantities and so was used for the standard run presented in the previous Section.

The interpretation of Figure 10 is straightforward: making the decoupling at smaller values of the drop radius has the effect of reducing the time interval during which the long range energy and momentum transfer away from the quark phase takes place. As a consequence, the specific entropy in the quark phase is changed less, leading to a smaller final compression. If the value of R_d/λ is taken to be very small, the hydrodynamical behaviour tends to the one observed when the decoupling is totally neglected and ultimately coincides with the solution obtained in [7] when $R_d/\lambda = 0$. This is a satisfying result and shows that the numerical modelling has an overall physical consistency.

Another example of this coherence appears when a self-similar solution can be recovered after decoupling between the radiation fluid and the standard fluids is complete. This can be produced if λ is artificially increased so as to be much larger than the length scale associated with the surface tension, thus separating the two possible regimes during which a compression can be produced.

Figure 11 shows the profiles of the compression factors immediately ahead of and behind the phase interface for values of $\lambda = R_d$ ranging between 10^4 fm (the physically realistic value) and 10^7 fm. (In all simulations the quark drop has initial dimensions $R_{s,0} = 10\lambda$.) It is evident that with the standard set of parameters, (shown with the continuous line), the two different compression growth stages join together and that self-similar evolution (represented by a constant compression factor state) cannot set in. The situation is rather different for the (unrealistic) choice of $R_d = \lambda = 10^7$ fm. In this case it is possible to distinguish clearly between the initial compression growth (produced by the relativistic radiative transfer), and the final

24

compression enhancement (a consequence of the accelerated evaporation driven by the surface tension) which in all of the simulations takes place for $R_s \lesssim 10^2$ fm. The evolution between the two stages clearly follows a self-similar solution and this seems to be a further example of the widespread occurrence of the self-similar solutions for an isolated contracting spherically symmetric system.

Figure 11. Compression factors immediately ahead of and behind the phase interface. Different curves refer to different values of the m.f.p. of the radiation fluid particles (expressed in fm) and show that if a large enough value is chosen, a self-similar evolution is reached. All curves are drawn for $R_d = \lambda$ and initial quark dimensions one order of magnitude larger than λ.

A final comment in this Section should be made concerning the role played by the neutrinos in the process of long range energy and momentum transfer away from the quark phase. As mentioned in Section II, neutrinos have been neglected in the present calculation because of the much larger length scale at which they interact ($\lambda_\nu \approx 10^{13}$ fm). Nevertheless, on this scale they can be considered as particles of a generalized radiation fluid and could operate a radiative transfer process similar to the one discussed so far for the electromagnetically interacting particles and produce a compressed hadron medium at the end of their decoupling.

In order to investigate the amplitude of this compression, we have performed a computation in which we simulate the decoupling between a radiation fluid composed only of neutrinos, and a standard fluid composed of strongly and electromagnetically interacting particles. It should be noted that this is a rather speculative investigation since it assumes the existence of isolated, spherical quark regions of dimensions at least comparable with λ_ν, and it is not clear whether the disconnection of quark regions happens at a scale large enough for this to occur. However, bearing this reservation in mind, results of our calculations for the effects of neutrino decoupling on the compression profiles are presented in Figure 12.

It is evident that entropy extraction by means of neutrinos is less effective than for the case of the electromagnetically interacting particles and this is the result of the different combination of the number of the degrees of freedom in the two cases (for neutrinos $g_r = 5.25$). Nevertheless, the decoupling produces a non negligible compression in both phases, giving a compression in the hadron plasma which is about five times greater than the background one.

25

Figure 12. Compression factors immediately ahead of and behind the phase interface. Here $R_d = \lambda_\nu = 10^{13}$ fm.

Reduction of α_1 would lead to further amplification of the compression in the same way as already discussed for the decoupling of the electromagnetically interacting particles. This result is also relevant for considerations of the baryon number density profile which is left behind by the quark-hadron transition and will be further discussed in the next Section.

VII.   Cosmological implications

We here briefly discuss some of the consequences that the results presented in the previous Sections can have in a cosmological context. A more detailed analysis of these features will be presented in a forthcoming paper [23].

A first question concerns the relation between the compression factor ρ in the two phases of the strongly interacting matter and the baryon number density which has a more direct physical relevance. Certainly, most of the astrophysical consequences which have been discussed in relation with a first order quark-hadron phase transition are connected with the production of baryon number inhomogeneities which could survive until later epochs. Baryon number density has a natural tendency to be discontinuous across the phase interface since baryon number is carried by almost massless quarks in the high temperature phase, while in the low temperature phase it is carried by heavy nucleons whose number density is strongly suppressed. In the limit of chemical equilibrium across the front, the baryon chemical potentials are equal for both phases of the strongly interacting matter, and the net baryon flow across the phase interface vanishes. If the evolution of the transition is isothermal with both phases at $\approx T_c$, the ratio of baryon number densities $k = (n_B^q/n_B^h)$ can be easily computed after having specified the critical temperature [22], with k being $\gtrsim 10$ for $T_c \lesssim 150$ MeV. The values obtained are slightly larger if the finite volume of the hadrons is not neglected [24].

This baryon number segregation can be further enhanced when the chemical equilibrium is broken (this could either occur because the interface velocity is much larger than the mean baryon diffusion velocity or because the bubbles have dimensions larger than the typical baryon diffusion scale length in a Hubble time $R_B^{diff} \sim 10^{10}$ fm). As a result of the breaking of chemical equilibrium, baryon number could accumulate on the quark side of the front. Depending on the intensity of

the net baryon number flow into the hadron region and on the efficiency of diffusion in smearing out accumulations of baryon number, the baryon density contrast can be magnified between 2 and 6 orders of magnitude [11, 12]. In addition to its relevance for cosmological nucleosynthesis, this mechanism has also been considered in connection with the possibility of it giving rise to primordial magnetic fields which could serve as seeds for the production of the present intergalactic and interstellar magnetic fields [13]. We here note that seed magnetic fields might also be produced at the very end of the transition when the quark drops evaporate rapidly and the radiative transfer favours baryon number segregation and hence charge separation [23].

The evolution of the baryon number contrast has been investigated by Kurki-Suonio [25] who considered several scenarios for the creation of the final baryon number density profile arising from various combinations of the intrinsic scale lengths of the problem: *i.e.* the baryon diffusion length, the mean separation of nucleation sites, and the typical dimension of hadron bubbles at coalescence. The last two length scales in particular, are still uncertain today and it has not yet been possible to clarify further the situation described in [25]. One of the scenarios considered by Kurki-Suonio was concerned with baryon number concentration produced by long range radiative transfer and, within this context, the results presented in the previous Sections can be used to provide an updated view of this. In the simplest picture where baryon number is taken to be strictly advected along with the hydrodynamical flow, the baryon number density is directly proportional to the compression factor ρ and so Figures 6–12 can be considered as representing also the baryon number density. However, departures from this proportionality can be caused both by diffusion of baryon number (which can operate when the typical length scale for variations in ρ is smaller than the relevant diffusion length scale or comparable with it), or by suppression of baryon number flow across the phase interface (which would lead to a build up of baryon number in the quark phase). It is expected that a filter mechanism would operate at the phase interface accumulating baryon number there and augmenting the concentration produced by the specific entropy extraction via the radiation fluid particles [22]. As a consequence, the results presented for the compression in the quark phase represent a lower limit to the possible enhancement of baryon number density in the high temperature phase.

As mentioned in Section VI, the scale length of the inhomogeneities produced by this mechanism is given by the m.f.p. for the radiative fluid particles and for the electromagnetically interacting particles this is much smaller than the minimum inhomogeneity scale length that can affect nucleosynthesis. An underlying large amplitude baryon number contrast would have to be produced during the intermediate

27

stages of the transition in order for the baryon number segregation produced to be on a large enough scale to be able to survive and be relevant for nucleosynthesis. This contrast might be achieved at the time of hadron bubble coalescence, or possibly during the decoupling of neutrinos from the standard fluids as discussed at the end of Section VI.

A final interesting issue to be investigated is the hydrodynamical evolution of the compression enhancements after the quark phase has been totally converted into the hadron one. Concentrating on a single quark drop, it is easy see that a rarefaction wave (possibly fronted by a spherical shock) should appear when the drop disappears [7, 27]. At this stage, the source of the outward flow from the quark phase ceases to exist and the flow profile should progressively deform as it moves out into the compressible hadron medium. As a result of this deformation, a shock front could be produced and this would then be followed by a region where the medium compressed by the shock is rarefied again to an equilibrium value. Given the energies and velocities, the it might well be that no shock appears or that there is only a rather weak shock which would damp rapidly. Independently of the fine details of the mechanism, the overall effect will be that of redistributing the excess energy and compression which was within the very small region of the disappearing quark drop. A numerical computation would be required to provide a full description of this process [23], but it is possible to make a rough estimate of the eventual degree of dilution of the compressed matter after the disappearance of the phase interface.

For this purpose, consider the sum of the enthalpy contained within a quark drop of radius $R_s \sim 1/T_c \sim 1$ fm

$$W \approx (e + p)_q \times \frac{4}{3}\pi T_c^{-3} = \frac{4}{3}\pi^2 g_q T_c^4 \times \frac{4}{3}\pi T_c^{-3} \approx 136.0 \text{ fm}^{-1}, \qquad (41)$$

and the surface energy

$$\Sigma \approx \sigma_0 T_c^3 \times 4\pi T_c^{-2} \approx 25.1 \text{ fm}^{-1}. \qquad (42)$$

Taking this to be converted into enthalpy of hadronic matter when the drop disappears, we then have an overdense region with enthalpy density

$$(e + p)' = \frac{(W + \Sigma)}{4/3\pi T_c^{-3}} \approx 307.5 \text{ fm}^{-4}, \qquad (43)$$

which will subsequently expand and come into equilibrium with the surrounding medium in which

$$(e + p)_h = 4g_h \pi^2 T_c^4 / 90 \approx 21.1 \text{ fm}^{-4}. \qquad (44)$$

If we make the assumption that the specific entropy of the material which was within the drop after the disappearance of the phase interface remains essentially unchanged, we then have $(e + p) \propto \rho^{4/3}$. In this case, compression dilution can be estimated to be

$$\frac{\rho_{fin}}{\rho'} = \left[\frac{(e+p)_h}{(e+p)'} \right]^{3/4} \approx \frac{1}{7.5} \tag{45}$$

where ρ_{fin} is the final compression factor of the fluid element and ρ' is its compression factor when the phase interface disappeared.

VIII. Conclusion

In this paper we have discussed the relativistic hydrodynamics of the very final stages of the cosmological quark-hadron phase transition. In particular, we have studied the evaporation of a single isolated spherical quark drop including the effects of long range energy and momentum transfer by means of electromagnetically interacting particles. This transfer takes place when the quark drop reaches dimensions which are comparable with the mean free paths of these particles and can lead to a significant modification of the hydrodynamical evolution (see [7] for comparison). For this study, a set of Lagrangian hydrodynamical equations for describing the evolution of the strongly interacting fluids has been coupled to an equivalent set of equations describing the hydrodynamics of the fluid of electromagnetically interacting particles. A numerical code has been constructed for integrating the complete set of equations and results from the computations have been presented.

The evolution of the quark drop starts by following the self-similar solution which characterizes an isolated spherical evaporating configuration and this behaviour is then broken when decoupling of the radiation fluid from the standard fluids takes place. A particular consequence of the long range energy and momentum transfer is the establishment of an entropy flux away from the quark phase carried by the long-m.f.p. particles of the radiation fluid. This acts so as to increase the compression of both phases of the standard fluid in the vicinity on the drop, producing overall relative increases of two orders of magnitude or more. Thus, even in the absence of suppression mechanisms operating at the phase interface, contrasts in the baryon number density of several orders of magnitude are natural products of a first order quark-hadron phase transition. The hydrodynamical properties of this process are completely general and similar results have been obtained when exploring the whole parameter space of the problem. In particular, it has also been shown

that larger compressions (up to seven orders of magnitude) can easily be achieved if the transparency of the phase interface to the hydrodynamical flux is decreased.

These computations, which are the first simulations of quark drop evaporation in the presence of radiative transfer, provide useful quantitative information about the final stages of the transition which can be used in studies of the evolution of baryon number inhomogeneities [23]. Density peaks of baryon number could be associated with the production of primordial magnetic fields, generated by the charge separation across the phase interface, and could possibly affect nucleosynthesis if produced over a large enough length scale.

Acknowledgments

References

[1] F. Karsch Nucl. Phys. B (Proc. Suppl.) **34**, 63 (1994)

[2] M. Crawford and D.N. Schramm, Nature, **298**, 538, (1982)

[3] Y. Iwasaki, K. Kanaya, L. Kärkkäinen, K. Rummukainen and T. Yoshié, Phys. Rev. D **49** , 3540 (1994)

[4] Y. Iwasaki, K. Kanaya, S.Kaya, S. Sakai and T. Yoshié in hbox*Lattice 94*, Proceedings of the International Symposium, Bielefeld, Germany, edited by F. Karsch *et al.* [Nucl. Phys. B (Proc. Suppl.) **42**, 499 (1995)]

[5] K. Kanaya, preprint UTHEP-296 (1995)

[6] Y. Iwasaki, K. Kanaya, S.Kaya, S. Sakai and T. Yoshié, preprint UTHEP-304 (1995)

[7] L. Rezzolla, J.C. Miller and O. Pantano, Phys. Rev. D **52**, 3202 (1995)

[8] L. Rezzolla and J.C. Miller, Class. Quantum Grav. **11**, 1815 (1994)

[9] J.C. Miller and L. Rezzolla, Phys. Rev. D **51**, 4017 (1995)

[10] K.S. Thorne, M.N.R.A.S. **194**, 439 (1981)

[11] C. Alcock, G.M. Fuller and G.J. Mathews Ap. J. **320**, 439 (1987)

[12] K. Jedamzik, G.M. Fuller, G.J. Mathews and T. Kajino Ap. J. **422**, 423 (1994)

[13] B. Cheng and A. Olinto, Phys. Rev. D **50**, 2421 (1994)

[14] L. Nobili, R. Turolla and L. Zampieri, Ap. J. **383**, 250 (1991)

[15] L. Nobili, R. Turolla and L. Zampieri, Ap. J. **404**, 686 (1993)

[16] K. Maeda, Gen. Rel. and Grav. **18**, 931 (1986)

[17] J.C. Miller and O. Pantano, Phys. Rev. D **40**, 1789 (1989)

[18] M. Gyulassy, K. Kajantie, H. Kurki-Suonio and L. McLerran, Nucl. Phys. B **237**, 477 (1984)

[19] S.A. Bonometto and O. Pantano, Phys. Rep. **228** 175 (1993)

[20] L. D. Landau and E. M. Lifshitz, *Fluid Mechanics*, Pergamon Press, Oxford, (1993)

[21] R. Courant and K.O. Friedrichs *Supersonic flow and shock waves*, Springer, New York (1976)

[22] G.M. Fuller, G.J. Mathews and C.R. Alcock Phys. Rev. D **37**, 1380 (1988)

[23] J.C. Miller, O. Pantano, and L. Rezzolla, In preparation

[24] S.A. Bonometto, P.A. Marchetti and S. Matarrese Phys. Lett. B **147**, 216 (1985)

[25] H. Kurki-Suonio, Phys. Rev. D **37**, 2104 (1988)

[26] J.H. Applegate, C.J. Hogan, and R.J. Scherrer Phys. Rev. D **35**, 1151 (1987)

[27] K. Kajantie and H. Kurki-Suonio, Phys. Rev. D **34**, 1719 (1986)
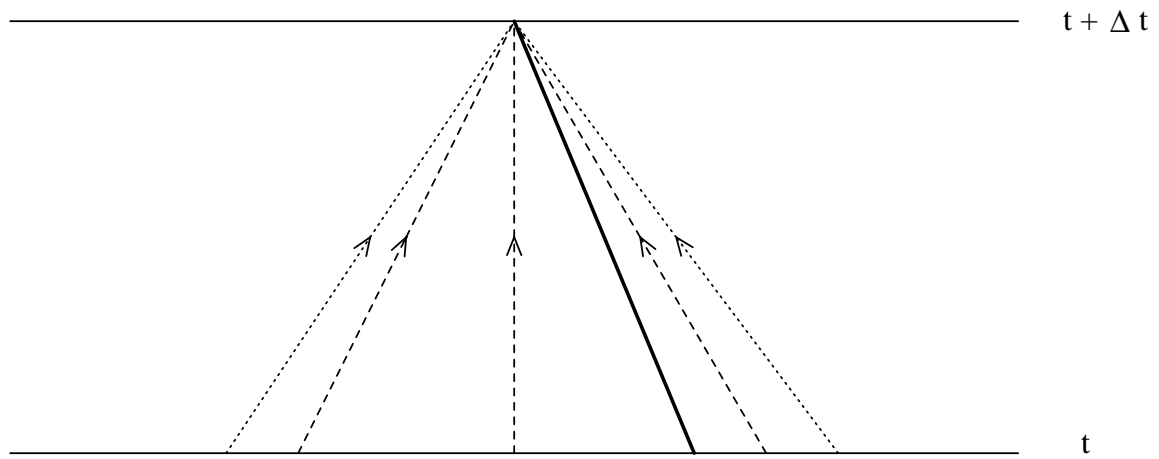
....	radiation fluid
- - - - - - -	standard fluid
——————	phase interface

$t + \Delta t$

t

R

$T_h/T_c=0.99, \ \sigma_0=1.00$

$\lambda=10^4, \ R_d=\lambda$

$T_h/T_c = 0.99$, $\sigma_0 = 1.00$

$\lambda = 10^4$, $R_d = \lambda$